Excitation-free quantum-state manipulation via Floquet engineering

Haoxuan Chen[1], Xiaosong Zhu[1], Pengfei Lan[1], Peixiang Lu[1], and Manfred Lein[2]

[1] Wuhan National Laboratory for Optoelectronics and School of Physics, Huazhong University of Science and Technology, Wuhan 430074, China

[2] Leibniz University Hannover, Institute of Theoretical Physics, Appelstr. 2, 30167 Hannover, Germany

E-mail: zhuxiaosong@hust.edu.cn and lein@itp.uni-hannover.de

April 2025

Abstract.

We present a non-adiabatic approach to transfer a quantum state between different superpositions of the eigenstates within a degenerate subspace, namely between eigenstates of various spatial orientations, while avoiding excitation. This is achieved by inducing different accumulated dynamical phases for the left- and right-rotating components of the state, in analogy with optical rotation. The control of the dynamical phase is based on the asymmetric Floquet energy shift induced by a monochromatic circularly polarized external laser field. In contrast to adiabatic control methods demanding an extremely slowly varying carrier wave of the laser field for excitation-free control, our approach requires only moderately slow variation in the envelope. This methodology promises fast quantum-state manipulation and control of electron dynamics in biological and chemical reactions.

Keywords: excitation-free; quantum-state manipulation; Floquet engineering.

Submitted to: *J. Phys. B: At. Mol. Phys.*

1. INTRODUCTION

The physics of controlling quantum states in quantum systems has received extensive attention in recent years, leading to numerous theoretical and experimental studies [1–18]. It plays an important role in quantum information science [19–27], quantum computing [28–37], and quantum communication [38–45]. A concomitant problem in quantum-state manipulation is excitation. The increase in excitation density can introduce disturbances, such as decoherence or noise, that interfere with the preparation and manipulation of quantum states, ultimately degrading the performance of quantum devices across various applications. To avoid this problem, adiabatic control is a possible way. The adiabatic process is slow enough so that the system remains always in an eigenstate of the time-dependent Hamiltonian, and thus there will be no excitation. However, the time required for this process will often be very long. A long time is detrimental, as it can also imply decoherence, accumulation of errors and perturbations, or even the escape of the system from its confinement. Moreover, with shorter process times, experiments could be repeated more often to increase signal-to-noise ratios. Therefore, there are ongoing efforts to achieve excitation-free quantum manipulation in a short time. A specific idea is to reach the final results of a slow adiabatic evolution through a shorter route. Consequently, the concept of "shortcuts to adiabaticity" (STA) was put forward [8] and various methods have been developed, such as the counterdiabatic or transitionless tracking approach [46], fast-forward approach [47, 48], alternative shortcuts through unitary transformations [49], and optimal control theory [50].

In quantum mechanics, it requires a much longer operation time to achieve adiabaticity when two or more degenerate states are involved. This is often the case when the parameters of the operation change in two dimensions rather than in one dimension. For a quantum system in an external laser field, for example, a linearly polarized driving field usually couples states of different energy, i.e., no degeneracies are involved. By contrast, a two-dimensional (2D) driving field will also couple the degenerate states at the same energy with different spatial orientations. We present a simple demonstration in the Appendix for clarity. The much longer time required with degenerate states can be understood as follows: Intuitively, an adiabatic process requires that the time scale for the parameter change, $\tau = 2\pi/\omega$, is much larger than $2\pi/\Delta\mathcal{E}$, with ω being the angular frequency of the driving field and $\Delta\mathcal{E}$ being the difference in energy eigenvalues of the involved states. Namely, it requires $\omega \ll \Delta\mathcal{E}$ (atomic units are used throughout this manuscript), although we note that strictly speaking the adiabaticity criterion is a much more complicated question [51–55]. When no degenerates states are involved, ω needs to be much smaller than the gap of different energy levels. However, when degenerate states are coupled, ω should be smaller than the difference between the shifted energies of the degenerate states after the degeneracy is lifted. Apparently, this requires a much smaller ω and thus a much longer driving period of the laser. Moreover, it is found that, if the external field crosses zero, the

process will converge to adiabaticity with decreasing of ω in a slower manner [51], adding to the requirement of a long operating time scale. Hence, developing a rapid method that overcomes the constraints of adiabatic conditions to transfer quantum states within the degenerate subspace is important for fields such as quantum control and quantum computation. Notably, different quantum states within the degenerate subspace exhibit different spatial orientations. The orientation of quantum states plays a critical role in microscopic dynamics such as chemical reactions and strong-field processes [11, 56]. Consequently, such control mechanisms are of paramount significance for manipulating the physical dynamics on ultrafast timescales.

In this work, we propose an excitation-free method that can manipulate quantum states in the degenerate subspace much faster than adiabatic processes, by using monochromatic circularly polarized light. The strategy is based on manipulating the dynamical phase of left- and right-rotating components of the state, owing to the asymmetric Floquet energy shifts of the components in the circularly polarized field. The scheme is numerically demonstrated by *ab initio* simulations and analyzed using Floquet theory. Our results show that excitation can be avoided with a driving pulse of only a few optical cycles. Besides, by adjusting the field parameters the final state can be freely adapted as required.

The paper is arranged as follows: In section 2 we briefly present the basic concept and theoretical framework. In section 3 and section 4, the numerical result is presented and we provide a detailed explanation of the mechanism behind this physical phenomenon. Finally, we summarize our findings in section 5.

2. Basic Concept

We consider an eigenstate of a quantum system, which has two degenerate states corresponding to the freedom of spatial orientation, as the initial state. We label the initial state as $|\psi_x\rangle$ and the degenerate state coupled by the 2D external laser field as $|\psi_y\rangle$. The subscripts x and y indicate that the two eigenstates have different spatial distributions. If we redistribute the population between $|\psi_x\rangle$ and $|\psi_y\rangle$, the finally obtained superposition of them $\cos\xi\,|\psi_x\rangle + \sin\xi\,|\psi_y\rangle$ is an eigenstate of the system, too, with the same eigenvalue and a different spatial distribution. Here, we choose ξ as real-valued and we write the coefficients as $\cos\xi$ and $\sin\xi$, because we consider the excitation-free control of the quantum state ($\cos^2\xi + \sin^2\xi = 1$).

One can consider an alternative set of basis set via the transformation

$$|\psi_+\rangle = \frac{1}{\sqrt{2}}(|\psi_x\rangle + i\,|\psi_y\rangle), \tag{1}$$

$$|\psi_-\rangle = \frac{1}{\sqrt{2}}(|\psi_x\rangle - i\,|\psi_y\rangle). \tag{2}$$

$|\psi_+\rangle$ and $|\psi_-\rangle$ are complex states with nonzero angular momenta and will be termed as left- and right-rotating states, respectively.

The initial state $|\psi_x\rangle$ can be written as a superposition of $|\psi_\pm\rangle$

$$|\psi_x\rangle = \frac{1}{\sqrt{2}}(|\psi_+\rangle + |\psi_-\rangle), \tag{3}$$

and also $|\psi_y\rangle = \frac{1}{\sqrt{2}i}(|\psi_+\rangle - |\psi_-\rangle)$. Therefore, any superposed state after the population redistribution can be written as:

$$\begin{aligned}\cos\xi\,|\psi_x\rangle + \sin\xi\,|\psi_y\rangle =& \frac{1}{\sqrt{2}}(|\psi_+\rangle\, e^{-i\xi} + |\psi_-\rangle\, e^{i\xi}) \\ =& \frac{e^{-i\xi}}{\sqrt{2}}(|\psi_+\rangle + |\psi_-\rangle\, e^{i2\xi})\end{aligned} \tag{4}$$

Equation (4) constitutes a pivotal conclusion of this study: the excitation-free population transfer between real eigenstates $|\psi_{x,y}\rangle$ with real coefficients is equivalent to controlling the relative phase between the complex states $|\psi_\pm\rangle$.

Hence, the next question is how to control the relative phases of the states without excitation. We will show that this can be achieved via Floquet engineering the energy level with a circularly polarized laser field. According to the Floquet theorem, with a time-dependent Hamiltonian $H(t) = H(t+T)$ that is periodic with period T, the time-dependent Schrödinger equation (TDSE) has solutions of the form $|\psi(t)\rangle = e^{-i\mathcal{E}_F t}\,|P(t)\rangle$ with $|P(t)\rangle = |P(t+T)\rangle$ known as Floquet states or dressed states. $\mathcal{E}_F$ is called the quasienergy. $\mathcal{E}_F$ and $|P(t)\rangle$ satisfy the Floquet equation

$$(H - i\partial/\partial t)\,|P\rangle = \mathcal{E}_F\,|P\rangle\,. \tag{5}$$

In our case, the period of the Hamiltonian is the period of the laser field, namely $T = 2\pi/\omega$. The shift of $\mathcal{E}_F$ compared to the energy for zero external field can be understood as the laser-dressing effect. In practice, the driving laser field has an envelope $f(t)$. If the initial state is a Floquet state and as long as the variation of the envelope is modest, the time-dependent state can be expressed as one Floquet state at each time. This leads to two consequences. First, the phase shift of the dressed state after the laser-matter interaction is

$$\varphi = -\int_{\text{pulse}} \mathcal{E}_F(t)dt. \tag{6}$$

The integration is performed over the duration of the laser pulse. $\mathcal{E}_F(t)$ can be time-dependent due to the variation of the envelope, and it is determined from the Floquet equation Eq. (5), where the amplitude of the laser-interaction term in H is determined by $f(t)$. Second, at the end of the laser pulse, the laser-dressed state becomes the Floquet state with zero external field. This state is the same as the initial Floquet state before the start of the pulse except for a phase shift according to Eq. (6). In essence, we have shown that Floquet engineering of the quantum system provides a method to control the phase of the state without excitation. Our discussion below will demonstrate that the requirement of a slowly varying envelope is easily fulfilled.

The ultimate task is to introduce different phase shifts for $|\psi_\pm\rangle$. Since the two states have opposite sense of rotation, they couple differently to a circularly polarized laser

field, and different shifts of $\mathcal{E}_F$ are expected. Consequently, the two states gain different dynamical phases and the relative phase between them can be effectively controlled.

3. Numerical example I: A three-level atomic system

3.1. Orbital evolution in a three-level TDSE

To demonstrate our concept, we provide numerical simulations and discussions for two example systems. In the first example, we consider a very simple model system: a three-level atomic system with two degenerate p_x and p_y states and one excited s state. The Hamiltonian of the system subject to the external laser field $\mathbf{E}(t)$, polarized in the $x-y$ plane, is given by $H(t) = H_0 + \mathbf{r}\cdot\mathbf{E}(t)$. Using the basis $(|p_x\rangle, |p_y\rangle, |s\rangle)$, $H(t)$ is written as

$$\begin{aligned} H(t) =& H_0 + \mathbf{r}\cdot\mathbf{E}(t) \\ =& \begin{bmatrix} \mathcal{E}_p & 0 & 0 \\ 0 & \mathcal{E}_p & 0 \\ 0 & 0 & \mathcal{E}_s \end{bmatrix} + \\ & \begin{bmatrix} 0 & 0 & E_x(t)\langle p_x|\, x\,|s\rangle \\ 0 & 0 & E_y(t)\langle p_y|\, y\,|s\rangle \\ E_x(t)\langle s|\, x\,|p_x\rangle & E_y(t)\langle s|\, y\,|p_y\rangle & 0 \end{bmatrix}. \end{aligned} \tag{7}$$

To proceed with specific numerical calculations, the eigenenergies and transition dipoles are set to the same values as in a widely used model Ne atom [57,58]. The corresponding energy level difference $\Delta\mathcal{E} = \mathcal{E}_s - \mathcal{E}_p$ and transition dipole moment $D = \langle s|\, x\,|p_x\rangle/\sqrt{2} = \langle s|\, y\,|p_y\rangle/\sqrt{2}$ are 0.576 a.u. and 0.463 a.u., respectively. The process is illustrated in Fig. 1(a), where the initial p state is driven by a monochromatic circularly polarized laser field. The electric field is written as $\mathbf{E}(t) = E_0 f(t)[\cos(\omega t)\hat{\mathbf{e}}_x + \sin(\omega t)\hat{\mathbf{e}}_y]$, where E_0 is the amplitude of the electric field and $f(t)$ is the envelope of the pulse. The envelope expression is $\sin^2(\pi t/T_{\text{all}})$ with T_{all} the full pulse width corresponding to 10 optical cycles from $t = 0$ to $t = T_{\text{all}}$. The $|p_\pm\rangle$ states will experience different energy shifts under the circularly polarized laser field [59–61].

The evolution of the state is obtained by numerically solving the TDSE. A typical result represented by the snapshots of the electron probability density (EPD) of the wave function at different times from $t = 0$ to $t = 10T$ is shown in Fig. 1(b). In this calculation, $E_0 = 0.08$ a.u. The wavelength of the driving laser field is 6000 nm corresponding to the laser frequency $\omega = 0.007594$ a.u. The real-space EPD is obtained as $\rho(x, y, t) = |\sum_j c_j(t)\psi_j(x, y)|^2$, where the index j ranges over the p_x, p_y, and s states. The superposition coefficients c_j are obtained from the TDSE. The real-space representations of the eigenstates $\psi_j(x, y)$ are the same as those in [57]. Comparing the EPDs of the initial state (at $t = 0$) and the final state (at $t = 10T$), the final state has the same dumbbell shape as the initial state except for a rotation of the state. The final state is an eigenstate of H_0 (the population on the s state is practically zero,

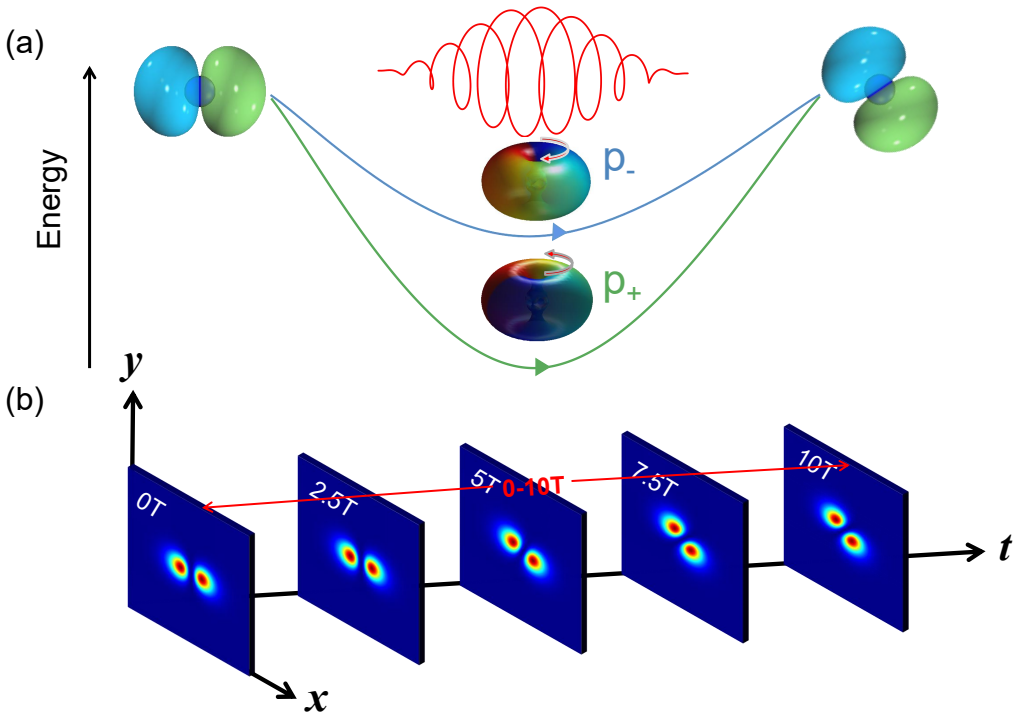

Figure 1. (a) Illustration of the strategy, taking the model atom of Sec. 3.1 driven by a laser field as an example. The $|p_\pm\rangle$ states experience different energy shifts under the circularly polarized laser field [59–61], resulting in a modification of the relative phase between the two states. As expressed by Eq. (4), modifying the relative phase between the two complex states $|p_\pm\rangle$ corresponds to the excitation-free population transfer between the real states $|p_{x,y}\rangle$, leading to a rotation of the spatial distribution of the superposition of $|p_\pm\rangle$. (b) Snapshots of the electron probability density from the TDSE simulation. The wavelength of the driving field is 6000 nm and the electric field amplitude is 0.08 a.u. As expected, the angle of the orbital rotates during the driving laser field.

see Fig. 2). The snapshots between $t = 0$ and $10T$ show the process during the light-matter interaction. We note that our goal is to transfer the initial state to another p eigenstate in the degenerate subspace *after* the operation. However, the time-dependent states during the interaction are not necessarily excitation-free eigenstates. Indeed, the process is not adiabatic, i.e., the time-dependent state during the interaction is not an eigenstate of $H(t)$.

Delving further into the process, we project the time-evolving wave function $|\psi(t)\rangle$ onto the complex basis states $|p_\pm\rangle$. The result is shown in Fig. 2(a) in a sphere similar to the Bloch sphere, which can well illustrate both the populations and phases for the p states. Specifically, we calculate $|c_{p_-}/c_{p_+}|$ and $\Delta\varphi = \arg(c_{p_-}) - \arg(c_{p_+})$ for $|\psi(t)\rangle$ at each moment, where $c_{p_\pm}(t) = \langle p_\pm|\psi(t)\rangle$. Then, the state $|\psi(t)\rangle$ is mapped to points on the spherical surface with polar angles $\theta_s = 2\arctan(|c_{p_-}/c_{p_+}|)$ and azimuth angles $\varphi_s = \Delta\varphi$. The latitude of the points indicates the relative population on $|p_\pm\rangle$ and the longitude indicates the relative phases for $|p_\pm\rangle$. As shown in Fig. 2(a), the initial state

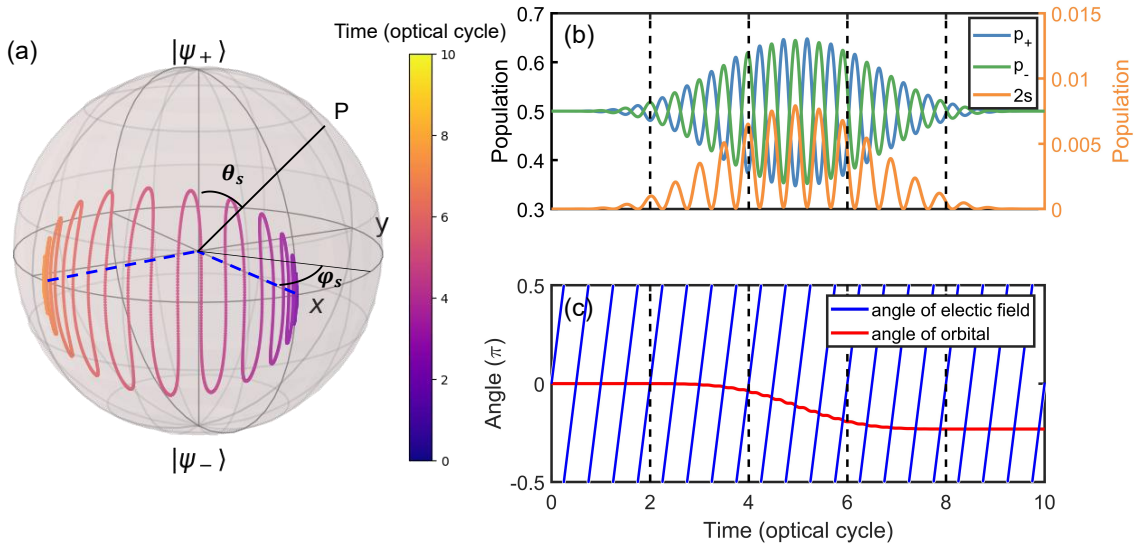

Figure 2. (a) Illustration of the time-evolving wavefunction on a sphere similar to the Bloch sphere (see the text in Sec. 3.1 for details). The parameters of the laser field are the same as those in Fig. 1. (b) The populations of p_+ (blue curve), p_- (green curve), and s states (orange curve) as a function of time. (c) The angles of the orbital ϕ (red curve) and the electric field (blue curve) as a function of time. The angles are wrapped into the interval $[-\pi/2, \pi/2]$.

$|p_x\rangle$ is at the intersection of the x-axis and the equator of the sphere. Then, the state evolves following the thick colored curve, oscillating around the equator. During this process, the state rotates from east to west with the longitude changing monotonically. This indicates that the relative phase between $|p_\pm\rangle$ gradually accumulates during the light-matter interaction as predicted in Sec. 2. After the interaction, the final state is still on the equator. The net effect of this operation is that the relative phase between $|p_\pm\rangle$ is changed while the populations remain equal. Namely, the final state has the same shape as the initial p_x state except for a rotation, as indicated by the two dashed blue lines.

To further confirm that no excitation is included in the final state after the process, the time-dependent populations of the three basis states ($|p_+\rangle$, $|p_-\rangle$, $|s\rangle$) are shown in Fig. 2(b). One can see that the final populations are equal to the initial ones and the population of the excited s state returns to zero at the end of the laser pulse. Thus, eventually no population is transferred from the p subspace to the excited state. According to Eq. (4), the change of the relative phase between $|p_\pm\rangle$ corresponds to a population transfer between $|p_{x,y}\rangle$.

To quantify the lack of excitation more intuitively, we calculate the fidelity of the final state with respect to the p eigenstates of the field-free Hamiltonian. We define the fidelity as $\mathcal{F} = \max_j\{|\langle\phi_j|\psi_{\text{final}}\rangle|^2\}$, where the index j ranges over all the eigenstates

in the p subspace. Namely, it is the maximum value among the squared moduli of the projections of the final state onto all the p eigenstates. The calculated result approaches 1 up to the seventh decimal place, indicating that the final state is still an eigenstate in the p subspace.

The orbital rotation angle ϕ has a very concise correspondence with the relative phase $\Delta\varphi$ between $|p_\pm\rangle$ as

$$\phi = \Delta\varphi/2. \tag{8}$$

A detailed derivation for this relation can be found in Appendix B. It holds even during the light-matter interaction when there is excitation to the s state. In this case, ϕ represents the rotation angle that characterizes the predominant direction of electron distribution relative to the x-axis. The obtained time-varying ϕ is plotted in Fig. 2(c) together with the transient angle of the laser field. The angles for both the orbital and laser field are wrapped into $[-\pi/2, \pi/2]$ as the alignment of the p orbital is the same for ϕ and $\phi + \pi$. One can see that the orbital is rotated gradually, while the electric field rotates fast with laser frequency ω. The asynchrony of the rotations clearly reflects that the laser-driven process is far from adiabaticity.

3.2. Numerical verification in Floquet theory

The key to our approach is the phase control of the states associated with the shift of quasienergies due to the external field. To further verify the physical picture of the phenomenon already shown by the TDSE simulation, we adopt the Floquet theory and calculate the quasienergy in the external fields. The quasienergy is obtained by solving the Floquet equation Eq. (5). As the laser pulse envelope $f(t)$ varies slowly compared to the carrier wave, we approximate the electric field around time t_0 as $\mathbf{E}(t; t_0) = E_0 f(t_0)[\cos(\omega t)\hat{\mathbf{e}}_x + \sin(\omega t)\hat{\mathbf{e}}_y]$, which is periodic in T. Moreover, considering the basis ($e^{-i\omega t}|p_+\rangle$, $e^{i\omega t}|p_-\rangle$, and $|s\rangle$) for the atomic state, the Floquet equation can be written as a matrix eigenvalue equation

$$H_F(t_0)|F\rangle = \mathcal{E}_F(t_0)|F\rangle \tag{9}$$

with the Floquet Hamiltonian [57]

$$H_F(t_0) = \begin{bmatrix} \mathcal{E}_p - \omega & 0 & DE_0 f(t_0) \\ 0 & \mathcal{E}_p + \omega & DE_0 f(t_0) \\ DE_0 f(t_0) & DE_0 f(t_0) & \mathcal{E}_s \end{bmatrix} \tag{10}$$

By solving Eq. (9) at various times t_0, the quasienergies for $p_\pm$ states (denoted as $\mathcal{E}_{F,\pm}$) varying over time are obtained. The numerical result is shown in Fig. 3(a). One can see that the quasienergies shift when the driving field is turned on. Importantly, the energy shifts for $p_\pm$ are different. As the amplitude of the external electric field increases, the quasienergy difference between $p_\pm$ also increases. According to Eq. (6), this energy

difference leads to an induced phase difference $\Delta\varphi$ between p_- and p_+ after passage of the laser pulse, given by

$$\Delta\varphi = -\int_{\text{pulse}} (\mathcal{E}_{F,-} - \mathcal{E}_{F,+})dt, \tag{11}$$

and the initial p orbital transformed into another one differing by the rotation angle

$$\phi = \frac{\Delta\varphi}{2} = -\frac{1}{2}\int_{\text{pulse}} (\mathcal{E}_{F,-} - \mathcal{E}_{F,+})dt. \tag{12}$$

In Fig. 3(b), we compare the angle predicted from Eq. (12) with that obtained from the TDSE simulation. The excellent agreement verifies that the excitation-free quantum control found in Sec. 3.1 is precisely based on the asymmetric Floquet engineering of the degenerate $p_\pm$ states in a circularly polarized external laser as we proposed.

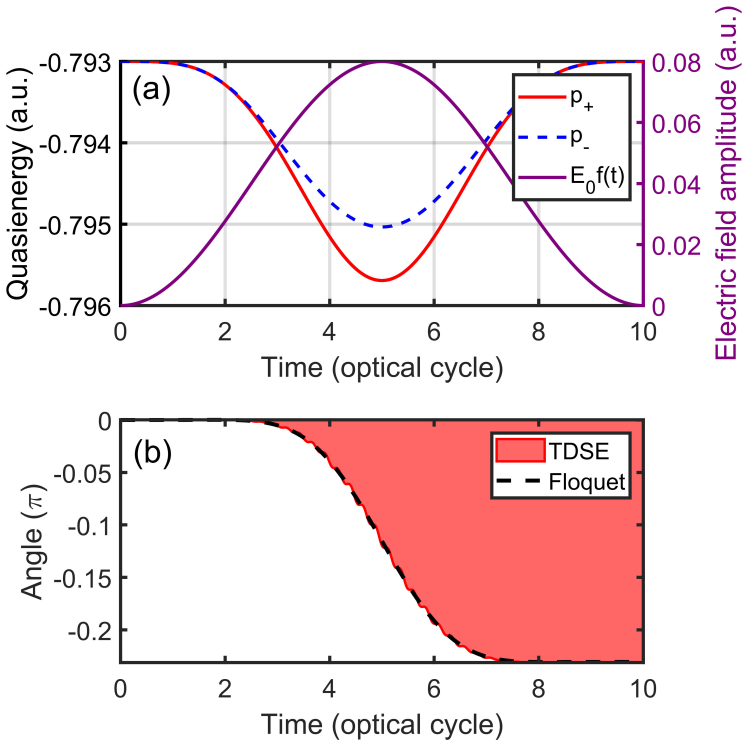

Figure 3. (a) Quasienergies of the laser dressed $p_\pm$ orbitals obtained from the Floquet theory as well as the amplitude of the electric field as a function of time. The laser parameters are the same as in Fig. 1. (b) The angle of the orbital obtained from Floquet theory (Eq. (12)) compared with that from numerically solving the three-level TDSE.

3.3. Controlling the states by tuning the laser intensity

As Eqs. (11) and (12) indicate, the relative phase and the rotation angle are determined by the difference of the laser-induced energy shifts. These depend on the intensity and wavelength of the driving laser field. Since it is easier to tune the intensity than the

wavelength, it will be an effective way to control the quantum state by adjusting the laser intensity.

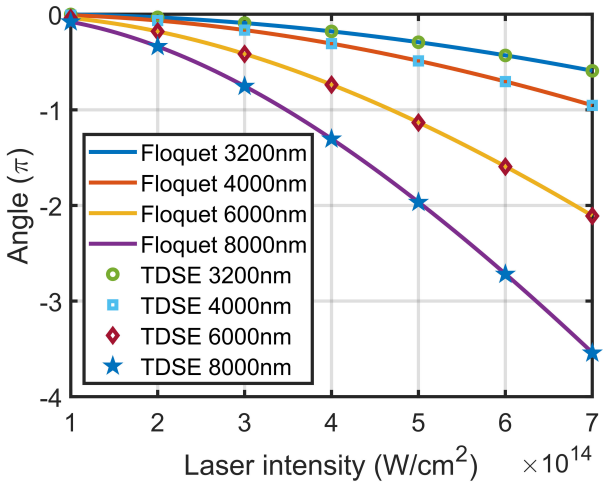

Figure 4. The orbital angle ϕ obtained from Floquet theory and by numerically solving the TDSE respectively for different laser wavelengths and intensities. The intensity varies from 1×10^{14} to 7×10^{14} W/cm^2 and the wavelengths are 3200, 4000, 6000, and 8000 nm.

As a demonstration, the rotation angles for various laser intensities and wavelengths obtained from both the TDSE simulation and the Floquet theory are displayed in Fig. 4. The other parameters are the same as in Fig. 2. Within almost an order of magnitude change in laser intensity, the results exhibit a smoothly monotonic dependence on intensity for various wavelengths. It is simple to predict the required input intensity for achieving the desired control after determining a few data points. Also, the good agreement between the TDSE and Floquet results again verifies the proposed physical picture.

Comparing our method with adiabatic processes, the adiabatic process generally requires that the angular frequency ω is much smaller than the difference between the shifted energies of the states after the degeneracy is lifted. Consequently, the wavelength needs to be on the order of tens of thousands of nanometers, corresponding to tens of femtoseconds per optical cycle. Therefore, the adiabatic process is impractical compared to our method.

4. Numerical example II: A non-isotropic system beyond three levels

Although the demonstration in Sec. 3 employs a simple 3-level atomic system, the fundamental idea is general. It is not restricted to 3-level systems, nor is it limited to isotropic systems. As a further numerical demonstration, we investigate the evolution of one of the degenerate highest occupied molecular orbitals (HOMO) of a borane molecule subject to a circularly polarized laser field, using real-space time-dependent

density functional theory (TDDFT) [62]. This system is planar and displays a threefold rotational symmetry. Besides, since the system is described in real space, it is not restricted to few levels.

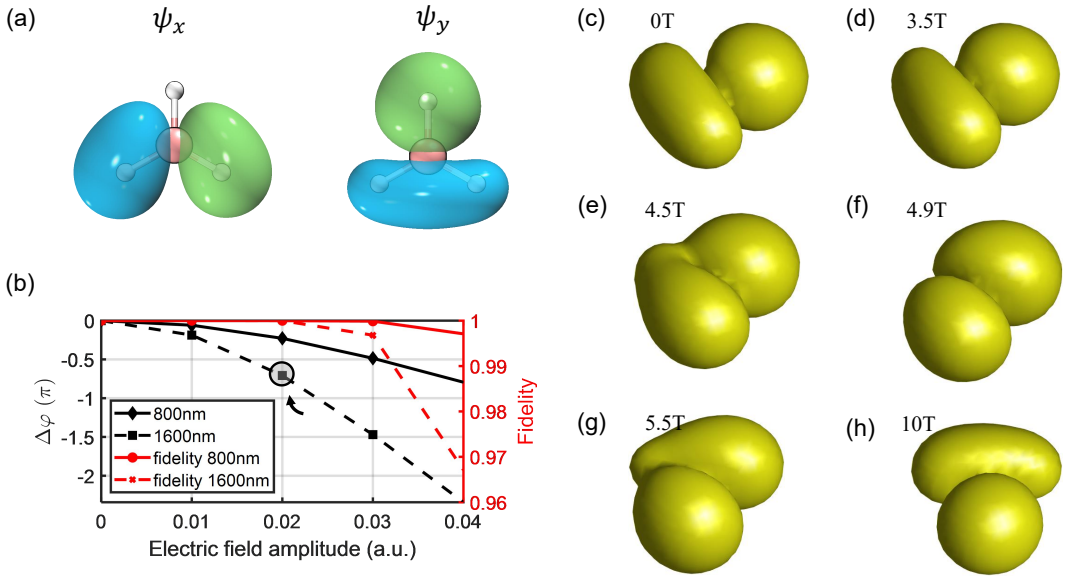

Figure 5. (a) The diagram of the molecular structure of borane and the degenerate HOMO orbitals ψ_x and ψ_y of the molecule. (b) The final relative phase $\Delta\varphi$ between the two degenerate states for different wavelengths (800 and 1600 nm) and different electric field amplitudes (0, 0.01, 0.02, 0.03, and 0.04 a.u.). The fidelities $\mathcal{F}$ of each case are shown by the dashed lines corresponding to the right vertical axis. (c) to (h) The electron probability density distribution over time from the TDDFT simulation with laser wavelength 1600 nm and electric field amplitude 0.02 a.u. as denoted by the arrow in panel (b).

The TDDFT computation is implemented using the open-access, real-space, and real-time code Octopus [63–65]. The Kohn-Sham (KS) equations are discretized on a Cartesian grid with spherical boundaries of radius 40 a.u. and the grid spacing is 0.4 a.u. The Boron atom is placed at the origin. The local density approximation (LDA) and Hartwigsen-Goedecker-Hutter LDA pseudopotentials are used for all atoms [66]. A diagram of the molecular structure of borane and the two degenerate HOMOs is shown in Fig. 5(a). The two HOMOs exhibit different spatial distributions and are denoted as ψ_x and ψ_y, respectively. In this numerical example, ψ_x is taken as the initial state. As mentioned in Sec. 2, one can also consider another set of orbitals via the transformation

$$|\psi_+\rangle = \frac{1}{\sqrt{2}}(|\psi_x\rangle + i\,|\psi_y\rangle), \tag{13}$$

$$|\psi_-\rangle = \frac{1}{\sqrt{2}}(|\psi_x\rangle - i\,|\psi_y\rangle). \tag{14}$$

$|\psi_+\rangle$ and $|\psi_-\rangle$ are complex states and will be termed as left- and right-rotating states respectively as in the atomic example. The initial state can be written as a superposition

of the two states with opposite rotations as $|\psi_x\rangle = \frac{1}{\sqrt{2}}(|\psi_+\rangle + |\psi_-\rangle)$. When driven by a circularly polarized laser pulse, different dynamical phase accumulations are obtained for $|\psi_\pm\rangle$ resulting in the excitation-free quantum control of the quantum state. The form of the applied laser field is the same as described above except for the intensity and wavelength. We consider various wavelengths (800 nm and 1600 nm) and different electric field amplitudes (0, 0.01, 0.02, 0.03, and 0.04 a.u.). Figure 5(b) shows the final phase difference between $|\psi_\pm\rangle$ after the laser-matter interaction as $\Delta\varphi = \arg[\langle\psi_-|\psi_{\text{final}}\rangle] - \arg[\langle\psi_+|\psi_{\text{final}}\rangle]$, where $|\psi_{\text{final}}\rangle$ is the final state at the end of the pulse. We find that $\Delta\varphi$ depends smoothly and monotonically on the intensity. The corresponding fidelity $\mathcal{F}$ is shown by the red lines corresponding to the right vertical axis in Fig. 5(b). The values are close to 1, indicating excitation-free control. Again, the change of $\Delta\varphi$ leads to effective control of the quantum state in the degenerate subspace, which corresponds to a rotation of the spatial distribution of the orbital. Figures 5(c)-(h) illustrate the electron probability density distribution over time from the TDDFT simulation, with laser wavelength 1600 nm and electric field amplitude 0.02 a.u. as denoted by the arrow in Fig. 5(b). These results for a non-isotropic system beyond three levels confirm the universality and reliability of our approach.

5. Conclusion

In summary, we propose a non-adiabatic approach for excitation-free control of quantum states. We first prove that the excitation-free population transfer between real eigenstates is equivalent to controlling the relative phase between the complex left- and right-rotating states. Then, we propose that Floquet engineering with a circularly polarized driving field introduces different phase shifts to the left- and right-rotating degenerate orbitals. During the interaction, the process is far from adiabaticity, thus the excitation-free operation with our method can be performed in a much shorter time scale than that required for an adiabatic process. The underlying picture and the feasibility of the method are numerically demonstrated based on the Floquet theory and by solving the TDSE. The results predicted by Floquet theory agree very well with the TDSE results, confirming the proposed physical mechanism. We also show that the phase shift and rotation angle can be effectively controlled by tuning the laser intensity. Finally, we show that the phenomenon is universal and we demonstrate a more general example without isotropic symmetry and beyond the single-active-electron approximation and few-level approximation. This technique opens new opportunities for quantum computing, the design of quantum gates, and the regulation of electron density in physical, chemical, and biological reactions.

Acknowledgement

H.C., X.Z., P. Lan, and P. Lu acknowledge support from the National Key Research and Development Program (Grant No. 2023YFA1406800) and the National Natural

Science Foundation of China (NSFC) (Grant Nos. 12174134 and 12021004). M.L. acknowledges support from the Deutsche Forschungsgemeinschaft (DFG, German Research Foundation) (Project No. 498967973). The computation was completed in the HPC Platform of Huazhong University of Science and Technology.

Appendix

A simple example comparing the processes in 1D and 2D external fields with degenerate states

Here, we apply the same atomic model as in Sec. 3.1. We first consider a 1D driving laser field linearly polarized in the x direction. Note that, although the degenerate states $|p_{x,y}\rangle$ are taken into account in this model, the laser field only couples the $|p_x\rangle$ and $|s\rangle$ states. Thus, one can roughly estimate that the process is adiabatic if the angular frequency of the driving laser is much smaller than the energy difference between the s and p levels $\Delta\mathcal{E} = 0.576$ a.u., i.e., the wavelength is much longer than 79.2 nm. Taking $|p_x\rangle$ as the initial state, we simulate the time evolution of the state in a monochromatic linearly polarized laser by numerically solving the TDSE. The intensity of the laser is 5×10^{14} W/cm^2 and the wavelength is 800 nm. In all the calculations in this appendix, the envelope of the laser pulses is sine squared with a full duration of 10 optical cycles. To quantitatively represent the state evolution, we calculate the dipole of the time-dependent state $|\psi(t)\rangle$ as $d(t) = -\langle\psi(t)|x|\psi(t)\rangle = -\int \rho(x,t)xdx$ with $\rho(x,t) = |\psi(x,t)|^2$. The time evolution of this quantity reflects the change of the electron density distribution in the external laser field. The result is shown in Fig. A1(a). The dipole changes periodically and synchronously with the electric field.

On the other hand, we examine the case of a 2D driving field, taking a counter-rotating bicircular polarized field as an example. The electric field is given by $\mathbf{E}(t) = [E_0\cos(\omega t) + E_1\cos(2\omega t)]\hat{\mathbf{e}}_x + [E_0\sin(\omega t) - E_1\sin(2\omega t)]\hat{\mathbf{e}}_y$, where E_0 and E_1 correspond to the intensities 5×10^{14} W/cm^2 and 5×10^{12} W/cm^2, and ω is the angular frequency of the fundamental component. The Lissajous figure of the field is shown in Fig. A1(b). We simulate the time evolution of the p_x initial state by numerically solving the TDSE. In this 2D case, the state evolution is represented by the angle of the predominant direction of electron distribution relative to the x-axis as in the main text. Figure A1(c) shows the result for the fundamental wavelength of 4000 nm. The time-dependent angle of the instantaneous electric field is shown as well. One can see that the angle of the state evolves in a totally different manner compared to the laser field, meaning that the evolution is far from adiabaticity. Figure A1(d) shows the results when increasing the fundamental wavelength to 28000 nm. Although the state rotates roughly following the electric field, the angle of the orbital still does not exactly coincide with the angle of the field, exhibiting additional oscillations. The evolution is still somewhat non-adiabatic with even such a long wavelength.

The comparison in Fig. A1 shows that a much longer wavelength is required for

the 2D driving field. This is because the 2D field also couples the degenerate p states. Consequently, the angular frequency of the driving field needs to be much smaller than the difference of the shifted energies of the degenerate states after the degeneracy is lifted to achieve adiabatic control, which is much more demanding than with a 1D driving field.

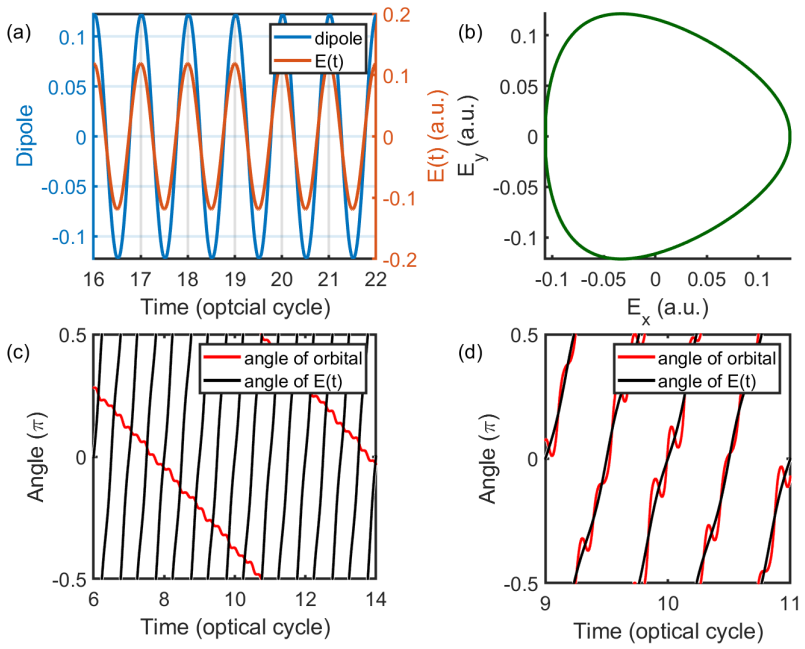

Figure A1. (a) The time-dependent dipole $d(t)$ of the orbital in a 1D driving field, where the intensity is $I = 5 \times 10^{14}$ W/cm^2 and the wavelength is 800 nm. (b) Lissajous figure of a counter-rotating bicircular field with 100:1 intensity ratio. (c) The time-dependent angle of the orbital ϕ in the 2D bicircular field with intensity and wavelength of the fundamental component being 5×10^{14} W/cm^2 and 4000 nm, respectively. The transient angle of the electric field is shown by the black curve. The angles are wrapped into the interval $[-\pi/2, \pi/2]$. (d) The same as (c) except that the fundamental wavelength is increased to 28000 nm.

Detailed proof of Eq. (8)

Here, we discuss the relationship between the rotation angle ϕ of the p orbital and the phase difference $\Delta\varphi$. In the coordinate representation, p_+ and p_- orbitals can be written as

$$\psi_{p_\pm}(\mathbf{r}) = \psi_0(r, \theta_r) e^{\pm i\varphi_r}, \tag{A1}$$

where r, θ_r, φ_r are the radial distance, polar angle, and azimuthal angle in the spherical coordinate system, respectively.

A superposition of the two states can be expressed as

$$\psi(\mathbf{r}) = |b_+|e^{i\alpha}\psi_{p+}(\mathbf{r}) + |b_-|e^{i\beta}\psi_{p-}(\mathbf{r}), \tag{A2}$$

where $|b_\pm|$ are the absolute values of the superposition coefficients while α and β are their phases. Substituting Eq. (A1) into Eq. (A2), we obtain

$$\begin{aligned} |\psi(\mathbf{r})|^2 &= |\psi_0(r,\theta_r)|^2 \\ &\times[(|b_+| - |b_-|)^2 + 4|b_+||b_-|\cos^2(\varphi_r - \frac{\Delta\varphi}{2})] \end{aligned} \tag{A3}$$

with $\Delta\varphi = \beta - \alpha$ the phase difference between $|p_\pm\rangle$. In Eq. (A3), $|\psi_0(r,\theta_r)|^2$ is independent of φ_r, the first term in the brackets is a constant and the second term maximizes at $\varphi_r = \Delta\varphi/2$, leading to a dumbbell distribution aligned along the direction $\Delta\varphi/2$.

For the final states after the excitation-free operation with the initial state p_x, we have $|b_\pm| = 1/\sqrt{2}$ and

$$|\psi(\mathbf{r})|^2 = 2\,|\psi_0(r,\theta_r)|^2\cos^2(\varphi_r - \frac{\Delta\varphi}{2}). \tag{A4}$$

This corresponds to a dumbbell p-orbital rotated by an angle of $\phi = \Delta\varphi/2$ relative to p_x. In particular, the orbital is p_x for $\Delta\varphi = 0$ and p_y for $\Delta\varphi = \pi$.

References

[1] Räsänen E, Castro A, Werschnik J, Rubio A and Gross E K U 2007 Physical Review Letters 98 157404
[2] Teranishi Y 2006 Physical Review Letters 97 053001
[3] Koll L M, Maikowski L, Drescher L, Witting T and Vrakking M J 2022 Physical Review Letters 128 043201
[4] Goodwin D L, Singh P and Foroozandeh M 2022 Science Advances 8 eabq4244
[5] Guéry-Odelin D, Ruschhaupt A, Kiely A, Torrontegui E, Martínez-Garaot S and Muga J 2019 Reviews of Modern Physics 91 045001
[6] Krantz P, Kjaergaard M, Yan F, Orlando T P, Gustavsson S and Oliver W D 2019 Applied Physics Reviews 6 021318
[7] Kues M, Reimer C, Lukens J M, Munro W J, Weiner A M, Moss D J and Morandotti R 2019 Nature Photonics 13 170–179
[8] Chen X, Ruschhaupt A, Schmidt S, Del Campo A, Guéry-Odelin D and Muga J G 2010 Physical Review Letters 104 063002
[9] Zanner M, Orell T, Schneider C M F, Albert R, Oleschko S, Juan M L, Silveri M and Kirchmair G 2022 Nature Physics 18 538–543
[10] Wollenhaupt M, Bayer T, Vitanov N V and Baumert T 2010 Phys. Rev. A 81 053422
[11] Liang J, Zhou Y, Liao Y, Jiang W C, Li M and Lu P 2022 Ultrafast Science 2022 9842716
[12] Boradjiev I I and Vitanov N V 2010 Physical Review A 82 043407
[13] Blekos K, Stefanatos D and Paspalakis E 2020 Physical Review A 102 023715
[14] Saadati-Niari M and Amniat-Talab M 2014 Journal of Modern Optics 61 1492–1499
[15] Amniat-Talab M, Saadati-Niari M, Guérin S and Nader-Ali R 2011 Physical Review A 83 013817

[16] Glaser S J, Boscain U, Calarco T, Koch C P, Köckenberger W, Kosloff R, Kuprov I, Luy B, Schirmer S, Schulte-Herbrüggen T, Sugny D and Wilhelm F K 2015 The European Physical Journal D 69 279
[17] Satzinger K J, Zhong Y P, Chang H S, Peairs G A, Bienfait A, Chou M H, Cleland A Y, Conner C R, Dumur Grebel J, Gutierrez I, November B H, Povey R G, Whiteley S J, Awschalom D D, Schuster D I and Cleland A N 2018 Nature 563 661–665
[18] Chen Y H, Qin W, Wang X, Miranowicz A and Nori F 2021 Physical Review Letters 126 023602
[19] Koch C P, Boscain U, Calarco T, Dirr G, Filipp S, Glaser S J, Kosloff R, Montangero S, Schulte-Herbrüggen T, Sugny D and Wilhelm F K 2022 EPJ Quantum Technology 9 19
[20] Brunner N, Cavalcanti D, Pironio S, Scarani V and Wehner S 2014 Reviews of Modern Physics 86 419–478
[21] Preiss P M, Ma R, Tai M E, Lukin A, Rispoli M, Zupancic P, Lahini Y, Islam R and Greiner M 2015 Science 347 1229–1233
[22] Liu X and Hersam M C 2019 Nauture Review Materials 4 669–684
[23] Brecht B, Reddy D V, Silberhorn C and Raymer M G 2015 Physical Review X 5 041017
[24] Islam R, Ma R, Preiss P M, Tai M E, Lukin A, Rispoli M and Greiner M 2015 Nature 528 77–83
[25] Pfaff W, Hensen B J, Bernien H, van Dam S B, Blok M S, Taminiau T H, Tiggelman M J, Schouten R N, Markham M, Twitchen D J and Hanson R 2014 Science 345 532–535
[26] Blais A, Grimsmo A L, Girvin S M and Wallraffe A 2021 Reviews of Modern Physics 93 025005
[27] Hucul D, Inlek I V, Vittorini G, Crocker C, Debnath S, Clark S M and Monroe C 2015 Nature Physics 11 37–42
[28] Gyongyosi L and Imre S 2019 Computer Science Review 31 51–71
[29] Cao Y, Romero J, Olson J P, Degroote M, Johnson P D, Kieferová M, Kivlichan I D, Menke T, Peropadre B, Sawaya N P D, Sim S, Veis L and Aspuru-Guzik A 2019 Chemical Reviews 119 10856–10915
[30] Jurcevic P, Javadi-Abhari A, Bishop L S, Lauer I, Bogorin D F, Brink M, Capelluto L, Günlük O, Itoko T, Kanazawa N, Kandala A, Keefe G A, Krsulich K, Landers W, Lewandowski E P, McClure D T, Nannicini G, Narasgond A, Nayfeh H M, Pritchett E, Rothwell M B, Srinivasan S, Sundaresan N, Wang C, Wei K X, Wood C J, Yau J B, Zhang E J, Dial O E, Chow J M and Gambetta J M 2021 Quantum Science and Technology 6 025020
[31] Northup T E and Blatt R 2014 Nature Photonics 8 356–363
[32] Saffman M 2016 Journal of Physics B: Atomic, Molecular and Optical Physics 49 202001
[33] Nigg D, Müller M, Martinez E A, Schindler P, Hennrich M, Monz T, Martin-Delgado M A and Blatt R 2014 Science 345 302–305
[34] Bruzewicz C D, Chiaverini J, McConnell R and Sage J M 2019 Applied Physics Reviews 6 021314
[35] Pogorelov I, Feldker T, Marciniak C D, Postler L, Jacob G, Krieglsteiner O, Podlesnic V, Meth M, Negnevitsky V, Stadler M, Höfer B, Wächter C, Lakhmanskiy K, Blatt R, Schindler P and Monz T 2021 PRX Quantum 2 020343
[36] Dumitrescu E, McCaskey A, Hagen G, Jansen G, Morris T, Papenbrock T, Pooser R, Dean D and Lougovski P 2018 Physical Review Letters 120 210501
[37] Barends R, Shabani A, Lamata L, Kelly J, Mezzacapo A, Heras U L, Babbush R, Fowler A G, Campbell B, Chen Y, Chen Z, Chiaro B, Dunsworth A, Jeffrey E, Lucero E, Megrant A, Mutus J Y, Neeley M, Neill C, O'Malley P J J, Quintana C, Roushan P, Sank D, Vainsencher A, Wenner J, White T C, Solano E, Neven H and Martinis J M 2016 Nature 534 222–226
[38] Zhang W, Ding D S, Sheng Y B, Zhou L, Shi B S and Guo G C 2017 Physical Review Letters 118 220501
[39] Hu J Y, Yu B, Jing M Y, Xiao L T, Jia S T, Qin G Q and Long G L 2016 Light: Science & Applications 5 e16144–e16144
[40] Muralidharan S, Li L, Kim J, L¨utkenhaus N, Lukin M D and Jiang L 2016 Scientific Reports 6 20463
[41] Zhou L, Sheng Y B and Long G L 2020 Science Bulletin 65 12–20

[42] Liao S K, Yong H L, Liu C, Shentu G L, Li D D, Lin J, Dai H, Zhao S Q, Li B, Guan J Y, Chen W, Gong Y H, Li Y, Lin Z H, Pan G S, Pelc J S, Fejer M M, Zhang W Z, Liu W Y, Yin J, Ren J G, Wang X B, Zhang Q, Peng C Z and Pan J W 2017 Nature Photonics 11 509–513
[43] Cozzolino D, Da Lio B, Bacco D and Oxenløwe L K 2019 Advanced Quantum Technologies 2 1900038
[44] Pittaluga M, Minder M, Lucamarini M, Sanzaro M, Woodward R I, Li M J, Yuan Z and Shields A J 2021 Nature Photonics 15 530–535
[45] Pirandola S, Laurenza R, Ottaviani C and Banchi L 2017 Nature Communications 8 15043
[46] Berry M V 2009 Journal of Physics A: Mathematical and Theoretical 42 365303
[47] Masuda S and Nakamura K 2008 Physical Review A 78 062108
[48] Masuda S and Nakamura K 2011 Physical Review A 84 043434
[49] Ibáñez S, Chen X, Torrontegui E, Muga J G and Ruschhaupt A 2012 Physical Review Letters 109 100403
[50] Salamon P, Hoffmann K H, Rezek Y and Kosloff R 2009 Phys. Chem. Chem. Phys. 11 1027–1032
[51] Zhu X, Lu P and Lein M 2022 Physical Review Letters 128 030401
[52] Born M and Fock V 1928 Zeitschrift für Physik 51 165–180
[53] Marzlin K P and Sanders B C 2004 Physical Review Letters 93 160408
[54] Tong D M, Singh K, Kwek L C and Oh C H 2005 Physical Review Letters 95 110407
[55] Amin M H S 2009 Physical Review Letters 102 220401
[56] Long J, Zhu X, Zhai C, Li W, He W, Lan P, He L and Lu P 2025 Ultrafast Science 5 0079
[57] Barth I and Lein M 2014 Journal of Physics B: Atomic, Molecular and Optical Physics 47 204016
[58] Medišauskas L, Wragg J, Van Der Hart H and Ivanov M Y 2015 Physical Review Letters 115 153001
[59] Herath T, Yan L, Lee S K and Li W 2012 Physical Review Letters 109 043004
[60] Zhu X, Lan P, Liu K, Li Y, Liu X, Zhang Q, Barth I and Lu P 2016 Optics Express 24 4196
[61] Wang D, Zhu X, Yuan H, Lan P and Lu P 2020 Physical Review A 101 023406
[62] Dreuw A and Head-Gordon M 2005 Chemical Reviews 105 4009–4037
[63] Castro A, Appel H, Oliveira M, Rozzi C A, Andrade X, Lorenzen F, Marques M A L, Gross E K U and Rubio A 2006 Physica Status Solidi (b) 243 2465–2488
[64] Andrade X, Strubbe D, Giovannini U D, Larsen A H, Oliveira M J T, Alberdi-Rodriguez J, Varas A, Theophilou I, Helbig N, Verstraete M J, Stella L, Nogueira F, Aspuru-Guzik A, Castro A, Marques M A L and Rubio A 2015 Physical Chemistry Chemical Physics 17 31371–31396
[65] Tancogne-Dejean N, Oliveira M J T, Andrade X, Appel H, Borca C H, Le Breton G, Buchholz F, Castro A, Corni S, Correa A A, De Giovannini U, Delgado A, Eich F G, Flick J, Gil G, Gomez A, Helbig N, Hübener H, Jestädt R, Jornet-Somoza J, Larsen A H, Lebedeva I V, Lüders M, Marques M A L, Ohlmann S T, Pipolo S, Rampp M, Rozzi C A, Strubbe D A, Sato S A, Schäfer C, Theophilou I, Welden A and Rubio A 2020 The Journal of Chemical Physics 152 124119
[66] Hartwigsen C, Goedecker S and Hutter J 1998 Physical Review B 58 3641–3662